

Vibrational modes of partly filled wine glasses

Gregor Jundt, Adrian Radu, Emmanuel Fort, Jan Duda, and Holger Vach^{a)}

Laboratoire de Physique des Interfaces et des Couches Minces, CNRS UMR-7647 - Ecole Polytechnique, 91128 Palaiseau, France

Neville Fletcher

Research School of Physical Sciences and Engineering, Australian National University, Canberra 0200, Australia

(Received 11 August 2005; revised 4 March 2006; accepted 29 March 2006)

Time-average holographic interferometry has been employed to study how the vibrational modes of a singing wine glass change when it is filled with a liquid. While the liquid clearly lowers the resonance frequencies, it does not change the vibrational mode structure in a first approximation. A more detailed analysis, however, reveals that the presence of the liquid causes the simultaneous excitation of two orthogonal modes that are well resolved for the empty glass. © 2006 Acoustical Society of America. [DOI: 10.1121/1.2198183]

PACS number(s): 43.40.Ey, 43.75.Kk, 43.20.Tb, 43.40.At [LPF]

Pages: 3793–3798

I. INTRODUCTION

It is a common game. You take a wine glass and you rub your moistened finger around its rim. Besides enjoying a generally rather pure tone emitted by your singing wine glass, you might even take pleasure in observing some ripples on the liquid surface that follow your rotating finger. On a less playful level, many famous composers such as Mozart, Berlioz, or Saint-Saëns have written master music pieces for instruments based on glass vibrations, also called “musical glasses.” The ethereal sound they produce has been much appreciated for many centuries. These instruments can be divided into two main groups depending on the way the vibrations are produced.¹ The first group is composed of percussion instruments like bells, cymbals, and balaphones made of glass. The second group consists of bowed instruments, like the glass harmonica and seraphim, that are excited by a “stick and slip” technique which is also at the origin of the sound production for our singing wine glass. The pitch can simply be tuned by pouring some liquid in the glass. This technique is, for instance, successfully used to tune seraph instruments. Another way to change the pitch is to use other glasses with a different thickness or diameter; glass harmonicas are commonly based on this second technique. The growing interest in glass musical instruments has already led to several papers on the acoustics of wine glasses.^{2–5} In this paper, we present experimental results obtained with simple wine glasses filled to various levels. We first show how the glass resonance frequencies vary with liquid quantity. Using time-average holographic interferometry, we then investigate the question whether the vibrational mode structure also becomes influenced by the presence of the liquid. We demonstrate that the latter one actually remains unchanged in a first approximation. A more detailed analysis, however, reveals that the liquid introduces an over-

lap of the two, previously well resolved, orthogonal mode frequencies leading to their simultaneous excitation.

In the next section, we describe our experimental setup. In Section III, we present a simple analytical model to explain the pitch lowering with increasing liquid quantity. Section IV is devoted to our experimental results and discussion.

II. EXPERIMENTAL SETUP

The experimental setup for holographic interferometry is shown in Fig. 1. The optical configuration we use for holographic recording is a modified Mach-Zehnder configuration. The laser beam originating from a 7-mW multi-mode He-Ne laser is split into two beams with equal intensities. The reference beam is filtered and expanded through a spatial filter consisting of a $\times 40$ microscope lens and a $10\ \mu\text{m}$ pin hole. The object beam is expanded by a diffuse glass and its length is chosen to equal the optical path length of the reference beam at the holographic plate in order to guarantee maximal temporal coherence. The position of the diffuser is chosen in such a way that the intensity of the reference beam is about three times higher than that of the object beam at the place of the holographic plate. In order to minimize vibrations the whole optical part is set on a properly isolated optical table. We determined the optimal exposure time to be about 50 s for our ABSYS BB-640 holographic plates. More experimental details concerning the holographic setup can be found in Refs. 6 and 7.

We placed a microphone approximately 2 cm below the glass rim and at a distance of about 2 mm from the glass. This microphone was then connected to a computer to record frequency spectra and to detect the resonance frequencies of the glass. The impulse response of the glass-liquid system was obtained by hitting the glass gently with a metal rod. The selective excitation of a particular vibrating mode was obtained by using a stabilized low frequency generator connected to the input of a 50-W amplifier with a loudspeaker. The accurate resonance frequency was obtained by comparing the amplitudes of the acoustic signal obtained for a

^{a)}Electronic mail: vach@leonardo.polytechnique.fr

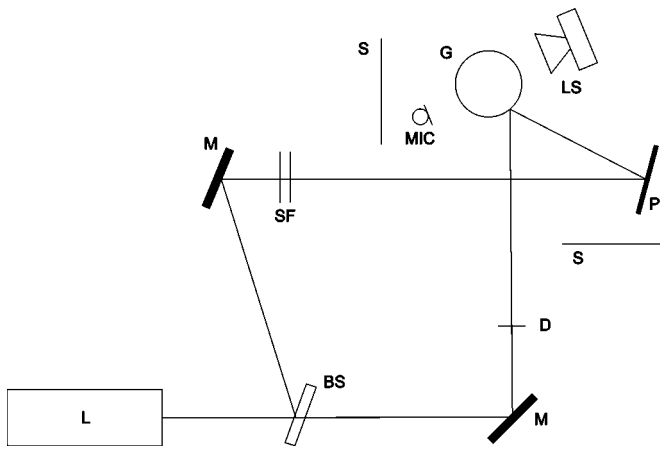


FIG. 1. Experimental setup for time-integrated holographic interferometry. L: laser, BS: beam splitter, M: mirror, SF: spatial filter, D: diffuse glass, MIC: microphone, LS: loudspeaker, P: holographic plate, G: wine glass, and S: beam stop against stray light.

clamped and an unclamped glass. Subtracting the acoustic response of the glass and the loudspeaker system from the one produced by the loudspeaker alone excited by a modulated sinusoidal signal gives an alternative method to obtain the acoustic response of the glass-liquid system. Both methods result in identical experimental resonance frequencies. Finally, the excitation of the quasi-degenerate (2,0) quadrupole modes⁴ can also be produced by the simple finger rubbing technique. In this case, however, the vibrational structure of the glass follows the exciting finger. Consequently, it becomes impossible to use time-average holographic interferometry with this excitation scheme. We chose, therefore, the excitation method with the metal rod only for the impulse response measurements while loudspeaker excitation was used for all the other experiments.

III. THEORY

A rigorous treatment of the vibration of liquid-loaded wine glasses is a complex matter for several reasons. Even for an empty glass, the profile is not simple and is different for every glass type: red-wine glasses, chardonnay glasses, champagne glasses, etc. In addition, the wall thickness varies progressively from relatively thick at the base to thin at the top edges. A solution for mode shape and frequency could, of course, be obtained for an arbitrarily shaped partly filled glass by using finite-element numerical analysis, but this would lead to specific rather than general understanding. The aim of the present analysis, in contrast, is to provide a simple treatment in which the underlying physics is made clear.

A. Fundamental mode

The shape of the wine glass under study is intermediate between that of a paraboloid of revolution clamped at its peripheral center, a cone clamped at its vertex, and a cylinder clamped around its base. Even the solution of these idealized cases is very complex,⁸ but our initial concern is only with the fundamental mode which is a simple elliptical deformation of the glass cross section, so that general approximations based on very simple considerations⁹ can be made. Suppose

that the tangential coordinate, measured from the base of the cup, is s , that the azimuthal coordinate is ϕ , and that the total length of the cup surface is L . The fundamental mode can then be written as

$$\psi(s, \phi, t) = f(s) \cos 2\phi \sin \omega t, \quad (1)$$

where ω is the angular frequency of the vibration and $f(s)$ is an unknown function of the coordinate s . To determine an approximation to this function we proceed as follows. The clamping constraint at the base requires that

$$f(0) = 0, \quad \left. \frac{\partial f}{\partial s} \right|_{s=0} = 0, \quad (2)$$

while the fact that the rim is free requires that

$$\left. \frac{\partial^2 f}{\partial s^2} \right|_{s=L} = 0, \quad \left. \frac{\partial^3 f}{\partial s^3} \right|_{s=L} = 0. \quad (3)$$

Since we are concerned here with the fundamental mode, which has no nodal rings, it is a good approximation to expand $f(s)$ as a power series and to retain only the first term, so that

$$f(s) \approx \frac{s^2}{L^2}, \quad (4)$$

which satisfies the condition (2) though not (3). Because of the other approximations necessarily involved in the analysis to follow, however, this will be regarded as adequate.

It is now necessary to convert the tangential coordinate s into a vertical coordinate z , and this depends in detail upon the shape of the glass. If the glass profile is cylindrical, then $z=s$ and there is no problem. Similarly for a conical glass $z=As \cos \theta$ where θ is the cone semi-angle and A is a constant. For a glass with parabolic profile, which is actually a closer approximation to the vessel studied, $z=As^2$ close to the base where the wall slope is small and more nearly $z=As$ higher up the glass where the slope is large. Since the real wine glass profile is somewhere between these extremes, and the glass thickness is not constant, an adequate approximation for the present purpose is to write the mode function $f(s)$ of (1) as z^β so that (1) becomes

$$\psi(z, \phi, t) \approx z^\beta \cos 2\phi \sin \omega t. \quad (5)$$

This approximate result can be compared with experiment by examining the positions of the fringes on the holograms of the vibrating glass surface and correcting for the local slope of the surface in the observation direction. This comparison is shown in Fig. 5, which will be discussed in detail in Sec. IV. The data are taken from two holograms made of a glass vibrating in the first and second modes, respectively. β does not depend on the scaling of the glass height. The plot indicates a best-fit value of $\beta \approx 2.1$ for the fundamental mode and $\beta \approx 3.6$ for the hexapolar (3,0) mode, which has three nodal diameters and no nodal circles.

In the next stage of the analysis it is assumed that addition of liquid to the glass does not have a significant effect upon the vibrational mode shape. This is the standard assumption of first-order perturbation theory. In a more accurate second-order perturbation treatment, the effect of the

liquid loading upon the mode shape would be included.¹⁰ This refinement is not attempted in the present case since the treatment already involves major approximations, so that undue mathematical refinement is not appropriate. It is, however, discussed briefly later.

In any simple harmonic vibration, the mean kinetic energy and elastic strain energy are equal. If it is assumed as a first approximation that the vibrational mode shape of the fundamental mode is independent of the liquid loading, then the elastic strain energy for a given amplitude can be assumed to have the constant value E and the kinetic energy of vibration of the glass walls the value $K\omega^2$, where K is a constant and ω is the vibration frequency. The kinetic energy of the contained liquid can be written $W\omega^2$, where W depends upon the depth h of the liquid in the glass and is proportional to the density of the liquid. From this it then follows that

$$\omega^2 = \frac{E}{K + W(h)}. \quad (6)$$

The form of the kinetic energy function $W(z)$ of the liquid depends upon the glass shape and the shape of the vibrational mode, both of which are complicated. To a reasonable approximation for the fundamental mode, however, this mode shape can be assumed to follow the mode shape of the glass walls as given by (5) with an additional two-dimensional internal flow of proportional amplitude. The mass of co-moving liquid at a given height z is proportional to the cross section $S(z)$ of the glass at that height, and so depends upon glass shape. The general expression for $W(h)$ is then

$$W(h) \propto \int_0^h S(z)z^{2\beta} dz \quad (7)$$

and we must evaluate the integral for each glass shape. For a cylinder, $S(z)$ is a constant independent of z , for a paraboloid of revolution $S(z) \propto z$, and for a cone $S(z) \propto z^2$, so that the integral in (7) is easily evaluated and has the form Bh^n where B is a constant depending upon the glass dimensions and $n = 2\beta + 1$ for a cylinder, $n = 2\beta + 2$ for a hemisphere, and $n = 2\beta + 3$ for a cone. Substituting this into (6) gives the result

$$\omega^2 = \frac{\omega_0^2}{1 + \alpha h^n}, \quad (8)$$

where ω_0 is the mode frequency for the empty glass, α is a constant proportional to the liquid density and also depending upon glass shape and wall thickness, and n is determined as discussed above.

Since the shape of the wine glass studied is complex, the theory can only predict approximate values for the parameter n . For a cylindrical glass $3 \leq n \leq 5$, for a paraboloidal glass $4 \leq n \leq 6$, and for a conical glass $5 \leq n \leq 7$, with the upper limit in each case being most nearly appropriate for a glass of uniform wall thickness. Since the shape most closely conforming to that of the experimental glass is paraboloidal, we expect to find that $n \approx 6$ gives the best fit to the experimental data, and indeed a value of $n = 5.5$, as shown in Fig. 2, does give an excellent fit.

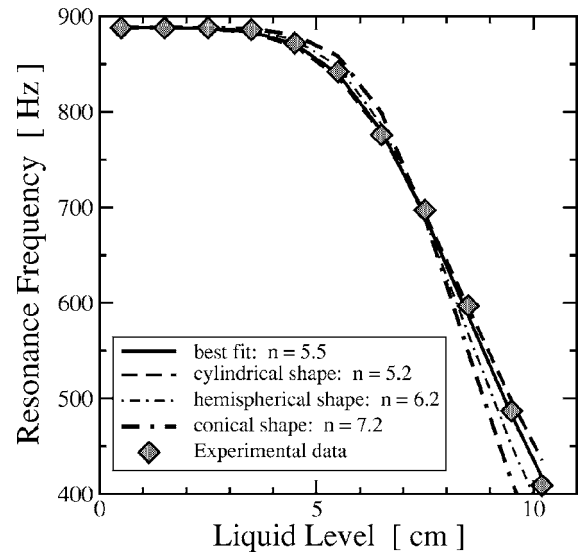


FIG. 2. Experimentally measured eigenfrequencies for the quadrupolar mode (2,0) as a function of water height. The dashed gray line results from the model for a cylindrical shaped shell while the black dotted line is the best-fit spherical curve and the gray continuous line the best-fit spherical-cap curve. The black continuous line shows the least-mean-square fit.

B. Higher modes

The analysis above considers only the fundamental mode which has two nodal diameters and no nodal circles. It is normal to refer to this as a (2,0) mode. A higher mode (p,q) with p nodal diameters and q nodal circles has the general form

$$\psi_{p,q}(s, \phi, t) = f_{pq}(s) \cos p\phi \sin \omega_{p,q}t, \quad (9)$$

and f_{pq} will generally increase about as s^p near the origin and then become oscillatory for larger values of s if $q \neq 0$. Such oscillations associated with the presence of nodal rings greatly complicate the analysis and experiment. If, however, there are no nodal rings, then the form of the mode function in (9) suggests that $\beta \approx p$ so that, since n in (8) lies between $2\beta + 1$ and $2\beta + 3$ and is actually about 5.5 from the experimental results for the (2,0) mode, we should expect values of about 7.5 and 9.5, respectively, for (3,0) and (4,0) modes.

There is another complication, particularly if many nodal diameters are involved, and this is that vibrations in the liquid will be increasingly localized near to the glass surface, so that the moving-mass term will increase more nearly as the glass perimeter rather than as its area. This has not been taken into account in the simplified analysis above.

C. Limitations of the present theory

Despite the success of this analysis in explaining the experimental results, it is useful to mention briefly the limitations of the predictions. In the limit of a fluid of infinite density, the second-order perturbation leading to changes in mode shape cannot be neglected, since the walls of the glass would be effectively clamped below the surface of the liquid. For the case of a partly filled glass this would lead to an increase in mode frequency with increasing liquid depth rather than a decrease. For this reversal of behavior to occur, it is necessary that the mass of the vibrating fraction of the

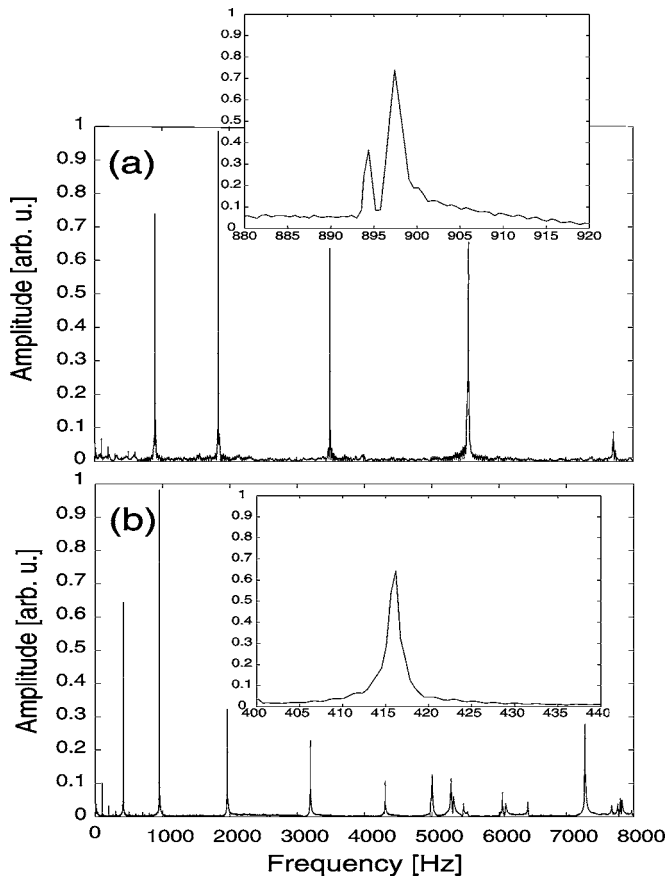


FIG. 3. Amplitude spectrum of the impulse response of an empty (a) and a full (b) glass. Insets: the associated orthogonal (2,0) modes.

liquid be very large compared with that of the vibrating walls. The determination of the threshold density above which this process reversal will take place certainly presents a challenging task for both experiments and theory, but clearly goes beyond the scope of our present work.

IV. RESULTS AND DISCUSSION

Figure 3 shows the typical spectra associated with an impulse response for the empty glass (a) and a glass filled with water (b). The insets show the spectra of the two orthogonal quadrupolar modes for each system. For the empty glass, only a few resonance frequencies are visible in the displayed spectrum. They can be attributed to the flexural $(m,0)$ modes with $m=2$ to 6.³ For a filled glass, the resonances are shifted toward lower frequencies. This is also true for higher modes. Therefore more resonance peaks appear within the frequency window of Fig. 3.

In the inset (a), the frequencies of the two orthogonal quadrupolar modes are clearly resolved for the empty glass, although the splitting is only about 4 Hz. This splitting is due to small imperfections in the glass structure (variation of thickness, presence of impurities, etc). In the case of a full glass [see inset of Fig. 3(b)], these two modes become degenerate. The reasons for this interesting result will be discussed in more detail below.

In Fig. 2, we present the measured resonance frequency for the (2,0) quadrupolar mode versus the water height in the

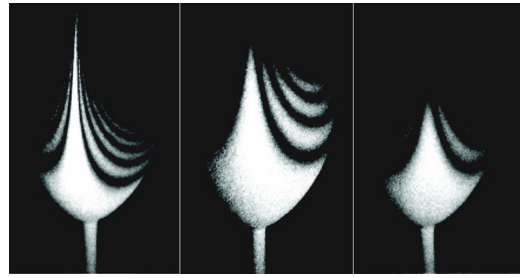


FIG. 4. Photographs of the holographic images of the vibrating wine glass: (a) empty, (b) half-filled with water, and (c) full. In all cases, the glass was excited by a loud speaker at the eigenfrequency of its quadrupolar (2,0) mode.

glass. While a careful parameter fitting might begin with $n \approx 6$ near the base and progress through $n \approx 5$ at medium heights to $n \approx 4$ near the top of the glass, such a refinement is not really justified, and we find a fit with $n \approx 5.5$ as being the most appropriate.

Figure 4 shows the photographs of the holographic images of the vibrating glass for three different filling levels: (a) empty, (b) half-full, and (c) full. The glass is always excited with the loudspeaker at the eigenfrequency of its quadrupolar (2,0) mode determined as described in Sec. II. The brightest fringe corresponds to the nodal line of the eigenmode in each hologram. Skeldon *et al.* showed glasses being intentionally broken by excitation (Fig. 10 in Ref. 4). The crack route most probably corresponds to an antinodal line where the bending stress is greatest. This line is displaced 90° from the nodal line for the case of the (2,0) vibration visible in our holograms.

From the number of fringes readily counted in Fig. 4, it is possible to deduce the vibrational amplitudes. Let the point M of the glass vibrate sinusoidally with an amplitude A and a pulsation ω in a direction toward the holographic plate. Its displacement is thus given by $x(M,t) = A(M) \sin(\omega t)$.

Since the exposure time $T \gg 1/\omega$, the intensity $I(M)$ of the reconstructed hologram is given by

$$I(M) \propto I_S(M) J_0^2 \left(\frac{4\pi}{\lambda} A(M) \right) \quad (10)$$

where $I_S(M)$ is the intensity of the reconstructed hologram scattered by the point M when it is not vibrating, J_0 is the Bessel function of the first kind of order zero, and λ is the light wavelength.⁶ Dark fringes are consequently centered at each point on the object surface where the Bessel function becomes zero for a given vibrational amplitude $A(M)$.

Figure 5 shows the vibrational amplitude normal to the surface of the empty glass f versus the height z . The data are calculated from the holograms taking into account the geometry of the incident beam and the observation direction. This analysis gives a regression of $z = Af^{0.47}$ for the fundamental mode. This implies that $\beta \approx 2.1$ which gives a value of n between 5 and 7, these extreme values being those for a cylinder and for a cone, respectively. Examining the shape of the glass used in the experiment, it is clear that, except for very small liquid levels such that $h < 0.3H$, where H is the total height of the glass cup, the glass profile is much more nearly cylindrical than conical, so that it is to be expected

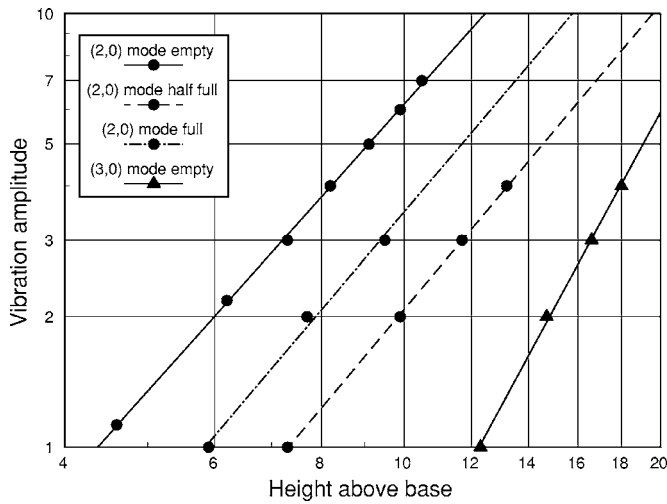


FIG. 5. Vibration amplitude $\psi(z)$ in units of $\lambda/2$, as measured by the progression of the bright fringes corrected for wall angle, plotted against height z above the base (in arbitrary units as measured from an enlarged photograph) for the fundamental (2,0) mode with different liquid levels and for the (3,0) mode. The straight lines are power-law regressions $\psi=Az^\beta$ as in Eq. (5). Note that the slope of all the (2,0) mode regressions is the same, indicating that addition of the liquid does not significantly modify the mode shape. Differing heights for corresponding bands for the (2,0) mode arise from different excitation efficiencies.

that the best-fit value of n will be closer to 5 than to 7. As shown in Fig. 2, the best-fit value derived from the microphone experiments is in fact about $n \approx 5.5$. The same analysis has been done for the (3,0) mode which leads to $\beta \approx 3.6$ and therefore $8.2 \leq n \leq 10.2$. This is in good agreement with the value $n \approx 8$ taken from the respective hologram.

About 25 dark fringes are visible in Fig. 4(a) which gives an approximate amplitude of $A_n \approx 4 \mu\text{m}$; for Figs. 4(b) and 4(c), $A_n \approx 1 \mu\text{m}$ (seven dark fringes) considering the employed recording geometry. The amplitude clearly decreases with the liquid level, presumably due to the increased inertia and the less efficient coupling of the loudspeaker to the glass as the frequency decreases.

The parameter α in Eq. (8) is proportional to the density of the liquid filled into the glass. In order to check formula (8) we measured the resonance frequencies for liquids with different densities. Figure 6 shows the data for liquids with three different densities, dichloromethane (1.32 kg/l), water (1 kg/l), and isopropanol (0.79 kg/l). From a fit according to formula (8) we obtain the ratios $\alpha_{\text{dichl}}:\alpha_{\text{water}}:\alpha_{\text{iso}} = 1:0.80:0.59$, which is in good agreement with the real density ratios of 1:0.75:0.60.

We can directly conclude from Fig. 4 that the presence of the liquid does not markedly modify the vibrational shape of the quadrupolar eigenmodes. It is, for instance, impossible to determine from the photographs up to which level the glass was filled. A plot of the positions of the bright fringes in the patterns of (b) and (c) of Fig. 4 for a partly and a completely filled glass using the logarithmic scale of Fig. 5 in fact gives straight lines closely parallel to that drawn for the (2,0) mode of an empty glass, showing that the assumption of little change in the vibrational mode function is justified. The main difference arising from the liquid is the fact that the nodal line no longer reaches the rim of the glass. In

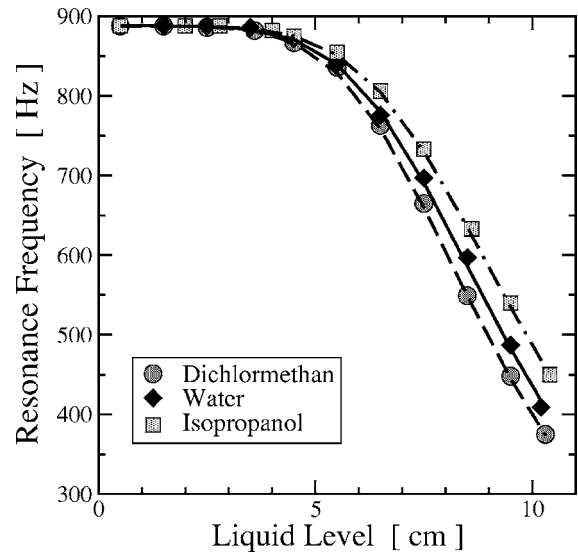


FIG. 6. The plot shows the resonances of the glass filled with dichloromethane, water, and isopropanol, respectively. The density of the liquid in use is proportional to the parameter α .

spite of the relatively high vibrational amplitude for the empty glass, the bright white nodal line clearly reaches the rim of the glass, while in the case of the half-full glass the upper part appears entirely dark. In the case of a completely filled glass, this phenomenon is even more pronounced. We attribute this effect to the fact that the coupling of the two degenerate modes should lead to an energy exchange between them. The resulting modulation of the vibrational modes, which is expected to have a frequency of a few Hz, however, darkens the image of the glass completely over the integration time of 50 s if the modulation amplitude is larger than $\lambda/2$.

Splitting of the resonances in degenerate modes, as shown in Fig. 3(a), is almost certainly due to asymmetry in the thickness of the glass so that the sine and cosine versions of Eq. (1) have slightly different frequencies. When liquid is added to the glass, this reduces the asymmetry because there is an equal liquid mass added to all parts of the wall. Consequently, the additional mass appears to shift the two resonance peaks to a point where the two nearly degenerate modes cannot be resolved anymore [compare Fig. 3(b)], leading to their simultaneous excitation. This phenomenon can also be nicely demonstrated by the use of the rotating finger excitation: The amplitude of the signal emitted by the empty glass as recorded with our microphone is strongly modulated since the excitation follows the finger. As the node passes in front of the microphone the amplitude becomes nearly zero when a sufficiently directional microphone is employed. When filled with water, however, the amplitude never vanishes entirely. Tentatively, we attribute this change in modulation amplitude to the simultaneous excitation of the two orthogonal quadrupolar modes which becomes possible due to the presence of the liquid. As a consequence, the coupled liquid-glass system clearly behaves differently from an empty glass. A similar behavior has already been reported for cylindrical steel tanks filled with water.¹¹⁻¹³

V. CONCLUSION

In conclusion, we showed that the presence of a liquid does not change the vibrational structure of a singing wine glass in a first approximation in spite of the obvious lowering of the resonance frequency, i.e., the vibrational movement of the glass continues nearly undisturbed below the level of the liquid. A more detailed analysis of our experimental results reveals, however, that the nodal line becomes modified near the glass rim: using time-average holographic interferometry, we showed how two well-resolved orthogonal quadrupolar modes of an empty glass become degenerate due to the presence of the liquid causing their simultaneous excitation.

ACKNOWLEDGMENTS

We would like to address our special thanks to Julien Masson and Professor Xavier Boutillon for fruitful discussions. We are grateful to the “Centre de Travaux Experimentaux de Physique - Ecole Polytechnique” where the holograms were recorded.

¹T. D. Rossing, “Wine glasses, bell modes, and Lord Rayleigh,” *Phys. Teach.* **28**, 582–585 (1990).

²A. P. French, “In Vino Veritas: A study of wineglass acoustics,” *Am. J. Phys.* **51**, 688–694 (1983).

³T. D. Rossing, “Acoustics of the glass harmonica,” *J. Acoust. Soc. Am.* **95**, 1106–1111 (1994).

⁴K. D. Skeldon, V. J. Nadeau, and C. Adams, “The resonant excitation of a wineglass using positive feedback with optical sensing,” *Am. J. Phys.* **66**, 851–860 (1998).

⁵A. Chaigne, “Le chant des verres de vin,” *Sciences et Avenir* **100**, 52–57 (1995).

⁶O. Haerberlé, B. Sapoval, K. Menou, and H. Vach, “Observation of vibrational modes of irregular drums,” *Appl. Phys. Lett.* **73**, 3357–3359 (1998).

⁷F. Pinard, B. Laine, and H. Vach, “Musical quality assessment of clarinet reeds using optical holography,” *J. Acoust. Soc. Am.* **113**, 1736–1742 (2003).

⁸W. Soedel, *Vibrations of Shells and Plates* (Marcel Dekker, New York, 1993).

⁹T. D. Rossing and N. H. Fletcher, *Principles of Vibration and Sound*, 2nd ed. (Springer-Verlag, New York, 2004).

¹⁰P. M. Morse and H. Feshbach, *Methods of Theoretical Physics* (McGraw-Hill, New York, 1953), Vol. **II**, Chap. 9.

¹¹P. G. Bentley and D. Firth, “Acoustically excited vibrations in a liquid-filled cylindrical tank,” *J. Sound Vib.* **19**, 179–191 (1971).

¹²C. R. Fuller and F. J. Fahy, “Characteristics of wave propagation and energy distributions in cylindrical elastic shells filled with fluid,” *J. Sound Vib.* **81**, 501–518 (1982).

¹³M. Amabili, “Vibrations of circular tubes and shells filled and partially immersed in dense fluids,” *J. Sound Vib.* **221**, 567–585 (1999).